



Curves and empirical formulas for predicting the diffraction field caused by edges of finite length

Penelope Menounou¹, Nikolaos Gkourlias¹, Petros Nikolaou¹

¹Department of Mechanical Engineering and Aeronautics, University of Patras, Patras, Greece
(email: menounou@upatras.gr)

Abstract

Curves and empirical formulas are presented that predict the diffraction field around finite length edges. Compared to analytical solutions, curves and formulas, although less accurate, reduce the computational time by orders of magnitude. They can, thus, be of interest for a range of applications that involve calculations of diffraction. A newly presented frequency domain solution is employed. It predicts the diffraction field around a finite length edge by an analytical expression that does not require numerical integration along the edge. Based on this expression, the SPL of the diffracted field around a finite length edge is compared to the SPL of the diffracted field around the corresponding infinitely long edge. The difference, ΔSPL , is reported as a family of curves dependent solely on two dimensionless parameters: the Fresnel number encountered in the study of diffraction by infinitely long edges and a second parameter specific to diffraction by finite length edges. The proposed family of curves can be thought of as a correction to the results obtained from existing methods (analytical or empirical) that predict the diffracted field around an infinitely long diffracting edge. Moreover, a family of curves and corresponding formulas are presented that can be used to estimate if a given finite length edge creates a diffraction field that approaches the diffraction field around an infinitely long edge (and thus no correction is needed).

Keywords: edge diffraction, finite length, chart

1 Introduction

The subject of the present work is sound diffraction by a finite length edge (see Fig.1) and the goal is to propose curves or empirical formulas that predict the diffraction field around the finite length barrier. Formulas and curves are less accurate than the analytical solutions, but require only a fraction of the computational time for their evaluation. This is essential, especially when the evaluation has to be performed thousands of times to predict the acoustic field around complex geometries with a large number of diffracting edges. A number of empirical formulas or curves exist for diffraction by infinitely long edges [1]-[4]. To the best of the authors' knowledge no empirical formulas or curves exist for finite length edges. The goal of the present work is to provide the correction that must be applied to results obtained from existing methods (analytical [5] [6] or empirical [1]-[4]) that predict the diffracted field around an infinitely long diffracting edge.

The analytical solution presented in ref [7] [8] is employed for the derivation of the curves and formulas. The analytical solution provides the diffracted field around a finite length edge in the frequency domain. As opposed to other analytical solution, it does not require a numerical integration along the edge of the barrier

and is applicable to all types of simple incident radiation (plane, cylindrically and spherically spreading incident waves).

Figure 1 shows the geometry of the source-edge-receiver problem. A cylindrical coordinate system is considered with its z-axis on the diffracting edge. The source is located at (r_s, ϕ_s, z_s) and the receiver is any point (r_R, ϕ_R, z_R) . The finite length edge is determined by the location of its end points on the z-axis, z_1 and z_2 . Each end point of the edge is associated with a *re-radiation time*. That is, the time sound needs to travel from the source to the end point of the edge and then to the receiver. The point Ξ on the z-axis ($z_\Xi = (r_s z_R + r_R z_s) / (r_R + r_s)$) is called *reference point* and is the point where the reference diffraction path $L = \sqrt{(r_R + r_s)^2 + (z_R - z_s)^2}$ (shortest distance sound travels to reach the receiver via diffraction on an infinitely long edge) intersects the z-axis. The lines SBI ($\phi_{SBI} = \pi + \phi_s$) and SBR ($\phi_{SBR} = \pi - \phi_s$) are called *shadow boundaries* and separate the sound field around the z-axis into three distinct regions: region I, II, and III. Associated with the shadow boundaries are the *diffraction delay times*

$$\tau_{lag}^{(i)} = \frac{L - R_1}{c}, \quad \tau_{lag}^{(r)} = \frac{L - R_2}{c}, \quad (1)$$

where $R_1 = \sqrt{r_R^2 + r_s^2 - 2r_R r_s \cos(\phi_R - \phi_s) + (z_R - z_s)^2}$ is the direct distance between source and receiver, $R_2 = \sqrt{r_R^2 + r_s^2 - 2r_R r_s \cos(\phi_R + \phi_s) + (z_R - z_s)^2}$ the distance between the image source and the receiver, and c the speed of sound. The diffraction delay time $\tau_{lag}^{(i)}$ represents the extra time the sound travels to reach the receiver by diffraction compared to the time it travels directly from source to receiver. Small values of $\tau_{lag}^{(i)}$ indicate receiver locations close to the shadow boundary SBI. Similarly, small values $\tau_{lag}^{(r)}$ indicate receiver locations close to the shadow boundary SBR. It is noted that the diffraction delay times are independent of the length of the edge.

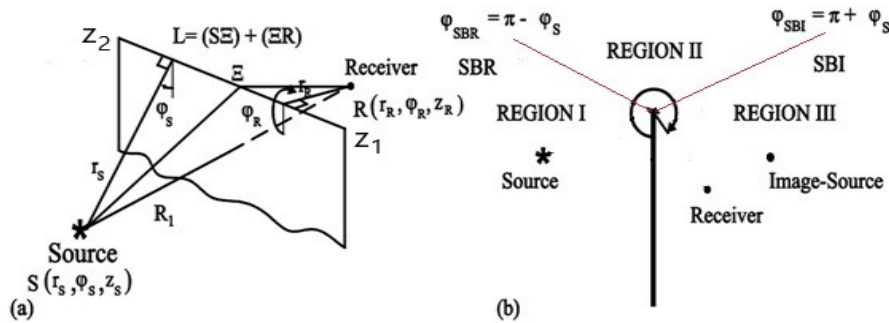


Figure 1 – Geometry of the problem.

2 Existing analytical solution and analysis of its terms

The employed analytical solution [7][8] has two different formulations: one when the reference point Ξ is located on the edge, and another one when the reference point is located outside the edge. For the analysis in the present work it is convenient to treat the two cases as shown in Figure 2. In the first case, the edge starts at the reference point and we will let its ending point move along the z-axis towards infinity, as the length of the edge increases. The relevant re-radiation time that is associated with the length of the edge is, therefore,

the re-radiation time through the edge's end point, or the *latest re-radiation time* τ_{end} . In the second case, the ending point of the edge is located at infinity and we will let its starting point move along the z-axis towards the reference point, as the length of the edge increases. Correspondingly, the relevant re-radiation time in this case is the re-radiation time through the starting point of the edge, or *earliest re-radiation time* τ_{start} . Because the finite length edges considered are restricted in the z-semi-axis, the results will be compared against the solution for a semi-infinitely long diffracting edge, instead of an infinitely long edge.

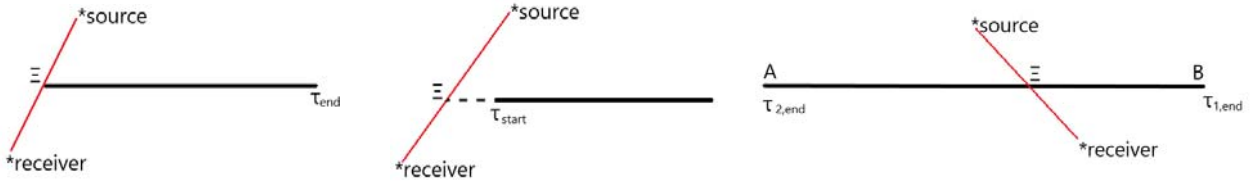


Figure 2 – Cases of finite length edge diffraction: reference point (Ξ) on the edge (left), reference point outside the edge (middle), edge extends on both sides of the reference point (right).

In the following we focus our attention to two properties of the analytical solution that will be employed in the present work. Firstly: Similarly to the analytical solution for the diffracted field around an infinitely long edge, the analytical solution for the diffracted field around a finite-length diffracting edge has two terms, one associated with the incident field and its parameters ($P_{d,finite}^{(i)}$) and one associated with the reflected field and its parameters ($P_{d,finite}^{(r)}$)

$$P_{d,finite} = P_{d,finite}^{(i)} + P_{d,finite}^{(r)} \quad (2)$$

Consider the case of the reference point being located on the edge. The two terms, $P_{d,finite}^{(i)}$, $P_{d,finite}^{(r)}$, as well as $P_{d,finite}$, are computed as the length of the edge increases (or equivalently as τ_{end} increases). Representative results are shown in Figure 3. It can be observed that as τ_{end} increases, all three computed quantities $P_{d,finite}^{(i)}$, $P_{d,finite}^{(r)}$ and $P_{d,finite}$ converge to fixed values (which correspond to the respective values for the semi-infinite edge). It can also be observed that $P_{d,finite}$ is closer to the term that has the smallest diffraction delay time. In the depicted case, $P_{d,finite}$ is closer to $P_{d,finite}^{(r)}$, as $\tau_{lag}^{(r)} < \tau_{lag}^{(i)}$. On the other hand, the pattern that $P_{d,finite}$ follows to converge to the semi-infinite solution seems to be the same with the term with the largest diffraction delay time, $P_{d,finite}^{(i)}$ in this case. The case of the reference point located outside the edge is also depicted in Figure 3. As expected, all computed quantities, $P_{d,finite}^{(i)}$, $P_{d,finite}^{(r)}$, and $P_{d,finite}$, approach zero, as the length of the edge decreases and moves further away from the reference point (or equivalently as τ_{start} increases). In this case, $P_{d,finite}$ is closer in value to the term that has the smallest diffraction delay time and has the same convergence pattern with the term that has the smallest diffraction delay time. In the depicted case, $P_{d,finite}$ is closer to and has the same pattern as $P_{d,finite}^{(r)}$, as $\tau_{lag}^{(r)} < \tau_{lag}^{(i)}$.

Secondly: Each one of the two terms $P_{d,finite}^{(i)}$, $P_{d,finite}^{(r)}$ is obtained from integration with respect to re-radiation time τ , which in turn is associated to the length of the edge. Specifically, the finite length edge is segmented logarithmically as follows: the re-radiation time of the beginning of each segment is 10 times smaller than the re-radiation time of the end of each segment, which is the beginning of the subsequent segment and so on. The integral along each such segment can be computed analytically as 4 different components. It has been numerically observed that the last one of these 4 components is the dominant contribution for each segment of the edge. The 4th component corresponding to segment j is approximated by the following expression:

$$\Lambda_4^{(i)(r)} = \frac{-e^{-\tau_{j-1}(d_j+i\omega)}}{(\tau_{j-1} + \tau_{lag}^{(i)(r)})(d_j + i\omega)} \quad (3)$$

where τ_{j-1} is the re-radiation time via the beginning of the j -th segment and d_j is a coefficient corresponding to segment j .

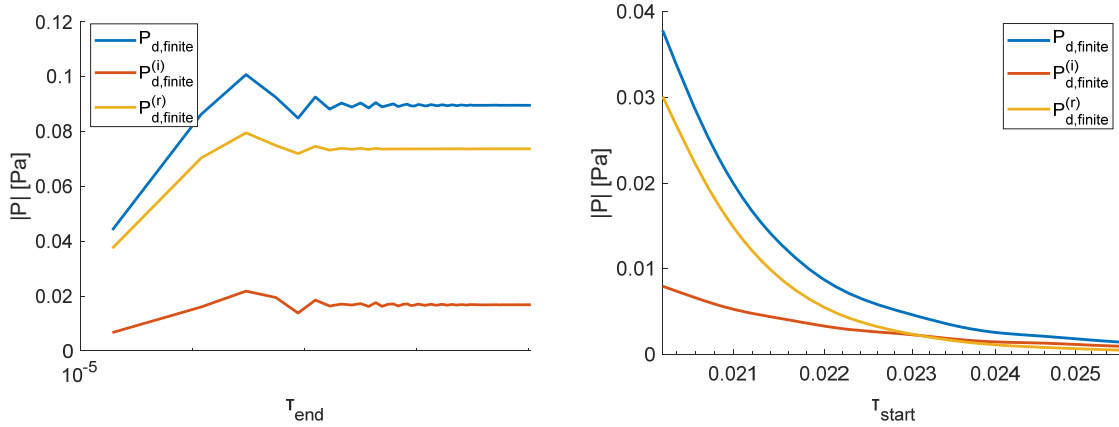


Figure 3 – The diffracted field due to finite length edge (the total diffraction field $P_{d,finite}$ and its terms $P_{d,finite}^{(i)}$ and $P_{d,finite}^{(r)}$) as a function of re-radiation time (left: reference point on the edge with $\tau_{lag}^{(r)} < \tau_{lag}^{(i)}$, right: reference point outside the edge with $\tau_{lag}^{(r)} < \tau_{lag}^{(i)}$)

3 Charts and equations to compute the transition from finite length to infinitely long edge diffraction

In this section we investigate under which conditions the diffraction field caused by a finite length edge approaches the diffraction field caused by an infinitely long edge. In such cases, the empirical formulas for infinitely long edges can be used and no correction due to the finite length of the edge is needed. Consider first the case of the reference point being on the edge. We wish to determine the critical τ_{end} , $\tau_{end,critical}$, for which the finite length edge behaves as an infinitely long edge. In this endeavour, we rely on the observation stated in section 2 that the 4th component of each segment of the edge provides the dominant contribution. Figure 4 shows this contribution, $|\Lambda_4|$, for each segment of the edge. The horizontal axis depicts the re-radiation times for the end points of each edge segment j . It can be observed that the segments close to the reference point (at beginning of the horizontal axis) provide small contributions. This is attributed to the logarithmic segmentation of the edge: the corresponding segments, although close to the reference point they have small lengths. Similarly, segments very far from the reference point provide also small contributions. The segments are large but are located far from the reference point, thus sound travels large distances to eventually reach the receiver. Intermediate segments provide the largest contributions.

As τ_{end} increases, we seek to find when the contributions $|\Lambda_4|$ become small enough (for example, 15% of its maximum value, $|\Lambda_4^{max}|$) and, thus, further increase of the length of the edge (or equivalently of τ_{end}) does not affect the diffracted field (i.e. the edge has become infinitely long):

$$|\Lambda_4| = \alpha |\Lambda_4^{max}| \quad (4)$$

where α a coefficient $0.1 < \alpha < 0.2$ Equation (4) can be solved analytically to provide the $\tau_{end,critical}$

$$\tau_{end,critical} = \frac{-d_j \max(\tau_{lag}^{(i)}, \tau_{lag}^{(r)}) - W_0(\beta)}{d_j} \quad (5)$$

$$\beta = \frac{-d_j e^{-d_j \max(\tau_{lag}^{(i)}, \tau_{lag}^{(r)})}}{a \sqrt{d_j^2 + \omega^2}} \quad (6)$$

where W_0 is the principal branch of the Lambert solution [9] and the parameter d_j is the coefficient of the segment, to which the critical re-radiation time corresponds. The critical re-radiation time is a function of frequency ($\omega = 2\pi f$) and diffraction delay time. It should also be recalled from section 2 that the delay time relevant to the convergence to the infinite edge is $\max(\tau_{lag}^{(i)}, \tau_{lag}^{(r)})$. The chart depicted in Figure 5 provides the $\tau_{end,critical}$ for any source – finite length edge – receiver configuration with known $\max(\tau_{lag}^{(i)}, \tau_{lag}^{(r)})$ and f .

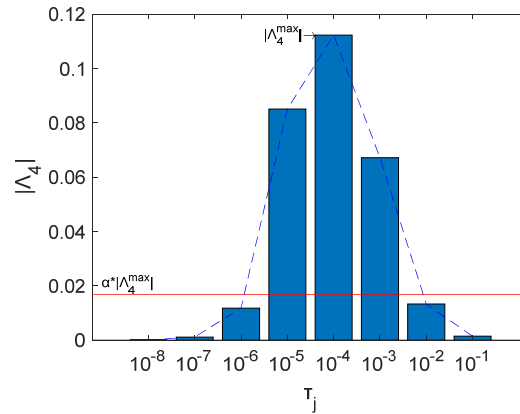


Figure 4 – The value of component $|\Lambda_4|$ versus the re-radiation time along the segments of the edge

Indeed, the critical re-radiation time $\tau_{end,critical}$ provided by the curves in Figure 5 is a reasonably good estimate as can be observed in Figure 6, where the critical re-radiation time is marked by the vertical red dashed line. For all frequencies, the predicted $\tau_{end,critical}$ marks approximately the re-radiation time, where the diffracted field caused by a finite length edge ($P_{d,finite}$) approaches the diffracted field by a semi-infinite edge.

The case of the reference point being outside the edge is considered next. Equation (5) remains the same, with the following differences: (i) $\min(\tau_{lag}^{(i)}, \tau_{lag}^{(r)})$ is chosen instead of $\max(\tau_{lag}^{(i)}, \tau_{lag}^{(r)})$ (see discussion in section 2), (ii) the critical segment is located before the segment where $|\Lambda_4|$ becomes $|\Lambda_4^{max}|$, (iii) for $j < 3$, the coefficient $d_j^2 \gg \omega^2$, the argument β of the Lambert solution becomes very small and its asymptotic form for small arguments can be used instead [9]. Equation (5), thus, becomes

$$\tau_{start,critical} = \frac{A + \ln(\alpha) - \left(A - \ln(A) + \frac{e}{e-1} \frac{\ln(A)}{A} \right)}{d_j \delta}, \quad (7)$$

where $A = -d_j \min(\tau_{lag}^{(i)}, \tau_{lag}^{(r)}) - \ln(\alpha)$ and $\delta = \ln(12000 - f)$ is an ad-hoc corrective factor. The chart depicted in the right column of Figure 5 provides the $\tau_{start,critical}$ for any source – finite length edge – receiver configuration when one knows the $\min(\tau_{lag}^{(i)}, \tau_{lag}^{(r)})$ and the frequency f . As expected, even if a small portion of

the edge around the reference point is missing from the diffracting edge, the diffracted field will not approach the diffracted field by the corresponding infinite edge. Similarly to Figure 6, Figure 7 shows that indeed the critical re-radiation time $\tau_{start,critical}$ provided by the curves in Figure 5 is a reasonably good estimate.

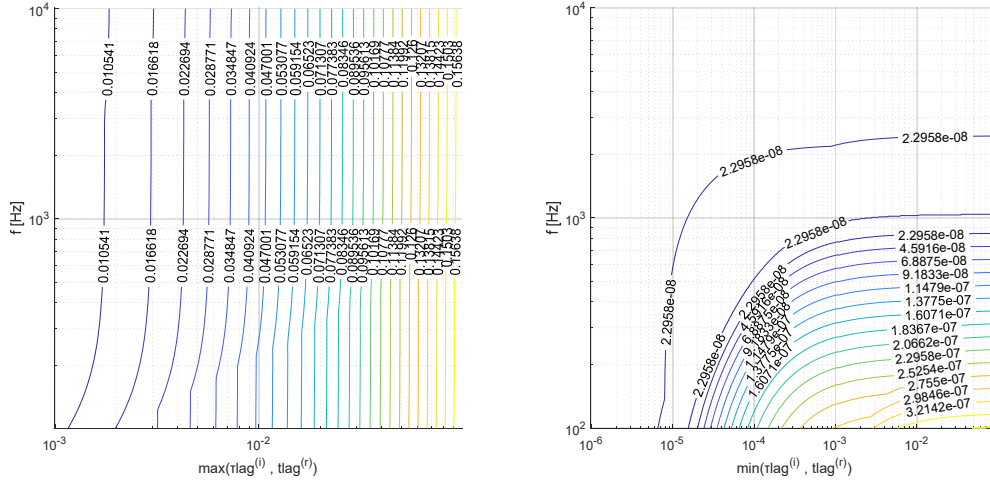


Figure 5 – Curves that provide the $\tau_{end,critical}$ (left) [$\tau_{start,critical}$ (right)] for any source – finite length edge – receiver configuration as a function of frequency f and of $\max(\tau_{lag}^{(i)}, \tau_{lag}^{(r)})$ (left) [$\min(\tau_{lag}^{(i)}, \tau_{lag}^{(r)})$ right] - reference point on the edge (left)[reference point outside the edge (right)]

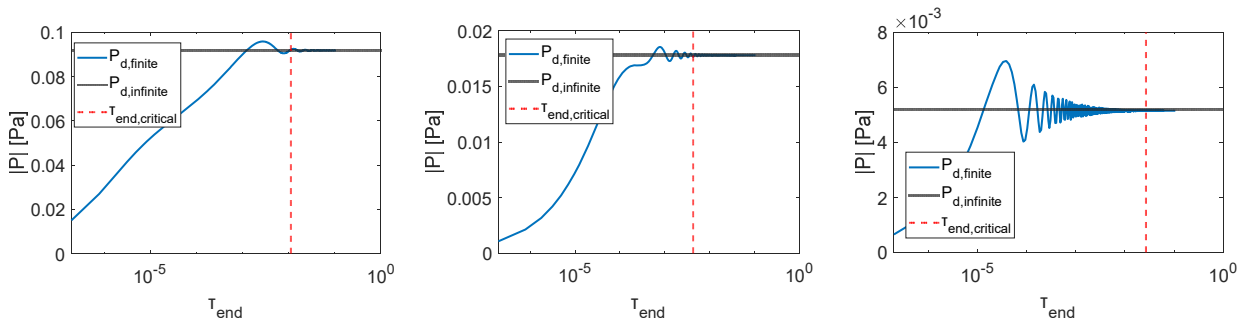


Figure 6– The critical re-radiation time $\tau_{end,critical}$ from the curves in Figure 5 mark reasonably well the point where the diffracted field from a finite edge approaches the diffracted field from a semi-infinitely long edge. for low (left), medium (middle) and high(right) frequencies

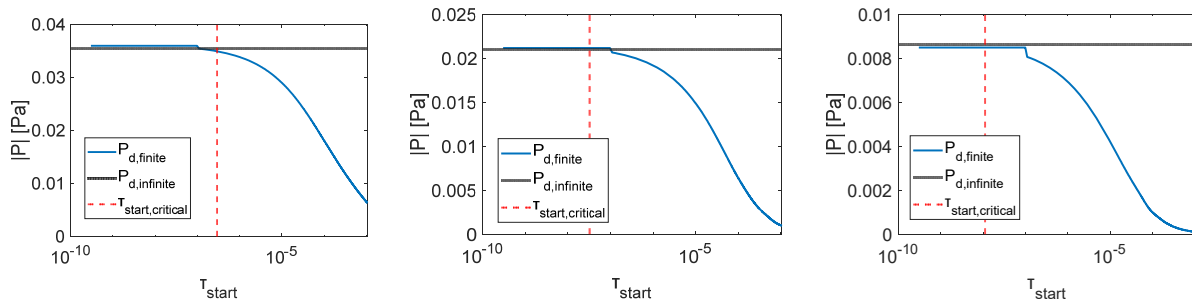


Figure 7 – The critical re-radiation times $\tau_{start,critical}$ from the curves in Figure 5 mark reasonably well the point where the diffracted field from a finite edge starts deviating from the diffracted field of a semi-infinitely long edge for low (left), medium (middle) and high(right) frequencies

4 Charts for computing the effect of the finite length of the edge

In this section charts are presented that provide the correction to the sound pressure level around a diffracting edge that must be applied because of the finite length of the edge. Specifically, curves will be presented that provide the difference

$$\Delta SPL^{(i),(r)} = SPL_{finite}^{(i),(r)} - SPL_{semi\ infinite}^{(i),(r)} \quad (8)$$

4.1 Universal parameters of the problem

Our investigation starts with an important numerical observation. The observation has a theoretical justification, which is, nevertheless, omitted in the present work. The parameters of the physical problem are nine: the frequency of the incident wave (f), the coordinates of the source location (r_s, ϕ_s, z_s), the coordinates of the receiver location (r_R, ϕ_R, z_R), and the location and length of the finite edge provided by the z-coordinates of the edge's ends, z_1 and z_2 . It was observed, however, that $\Delta SPL^{(i)}$ depends on only two parameters:

$$\omega \tau_{lag}^{(i)}, \frac{\tau_{end}}{\tau_{lag}^{(i)}} \quad (9)$$

Similarly, $\Delta SPL^{(r)}$ depends on $\omega \tau_{lag}^{(r)}$ and $\tau_{end} / \tau_{lag}^{(r)}$. The first parameter $\omega \tau_{lag}^{(i)}$ is associated with diffraction by infinitely long diffracting edges and is related to the Fresnel numbers [10], while the second parameter $\tau_{end} / \tau_{lag}^{(i)}$ is unique to diffraction by finite-length edges. It is further noted, that the dependence on two parameters can be observed in both cases: reference point on the edge, as well as, outside the edge. The left column of Figure 9 shows two completely different source-finite edge-receiver configurations, which, nevertheless, have the same universal parameter $\omega \tau_{lag}^{(i)}$, i.e. $\omega \tau_{lag,1}^{(i)} = \omega \tau_{lag,2}^{(i)}$. It can be observed that the deviation of the sound pressure level from the corresponding semi-infinitely long diffracting edge ($\Delta SPL^{(i),(r)}$) for these different configurations has exactly the same dependence on the normalized latest re-radiation time $\tau_{end} / \tau_{lag}^{(i)}$ (i.e. on the normalized length of the diffracting edge). Indeed, for the same normalized latest re-radiation time $\tau_{end,1} / \tau_{lag,1}^{(i)} = \tau_{end,2} / \tau_{lag,2}^{(i)}$, the value of $\Delta SPL^{(i),(r)}$ for both configurations is exactly the same. The same observations can be made for cases where for reference point is outside the edge (see the right column of Figure 9)

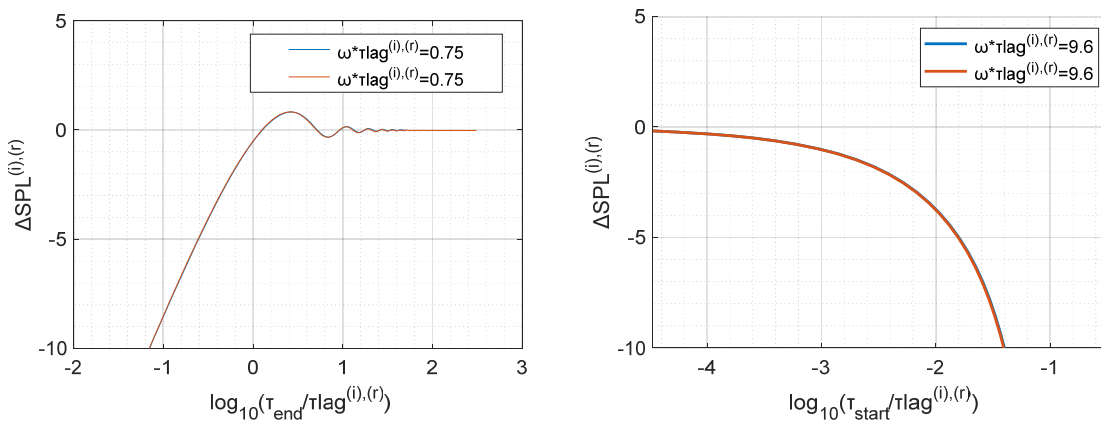


Figure 8 – The correction due to the finite length of the edge $\Delta SPL^{(i),(r)}$ is the same for different source-finite length edge-receiver configurations if they have the same $\omega \tau_{lag}^{(i),(r)}$ and $\tau_{end} / \tau_{lag}^{(i),(r)}$ (left: reference point on the edge, right: reference point outside the edge).

4.2 Curves for the effect of the finite length of the edge

The case of the reference point being on the edge is considered first. The left column of Figure 10 depicts the family of curves that provide the correction due to the finite length of the edge, $\Delta SPL^{(i)(r)}$, versus the normalized latest re-radiation time of the finite length edge ($\tau_{end}/\tau_{lag}^{(i)(r)}$) for various $\omega\tau_{lag}^{(i)(r)}$. It is noted that for high frequencies $\omega\tau_{lag}^{(i)(r)}$ the corrections have a highly oscillatory behaviour with respect to the re-radiation time (or equivalently the length of the edge), while for low frequencies the oscillatory behaviour does not appear. Also, it is noted that, as expected, the correction approaches zero as the length of the edge increases.

The right column of Figure 10 regards the case of the reference point being outside of the edge. The Figure depicts the family of curves that provide the correction due to the finite length of the edge, $\Delta SPL^{(i)(r)}$, versus the normalized earliest re-radiation time of the finite length edge ($\tau_{start}/\tau_{lag}^{(i)(r)}$) for various $\omega\tau_{lag}^{(i)(r)}$. It is noted that as τ_{start} increases, the missing portions of the edge close to the reference point increase, and as a result the diffracted field decreases and increasingly deviates from the diffracted field from a semi-infinitely long edge,

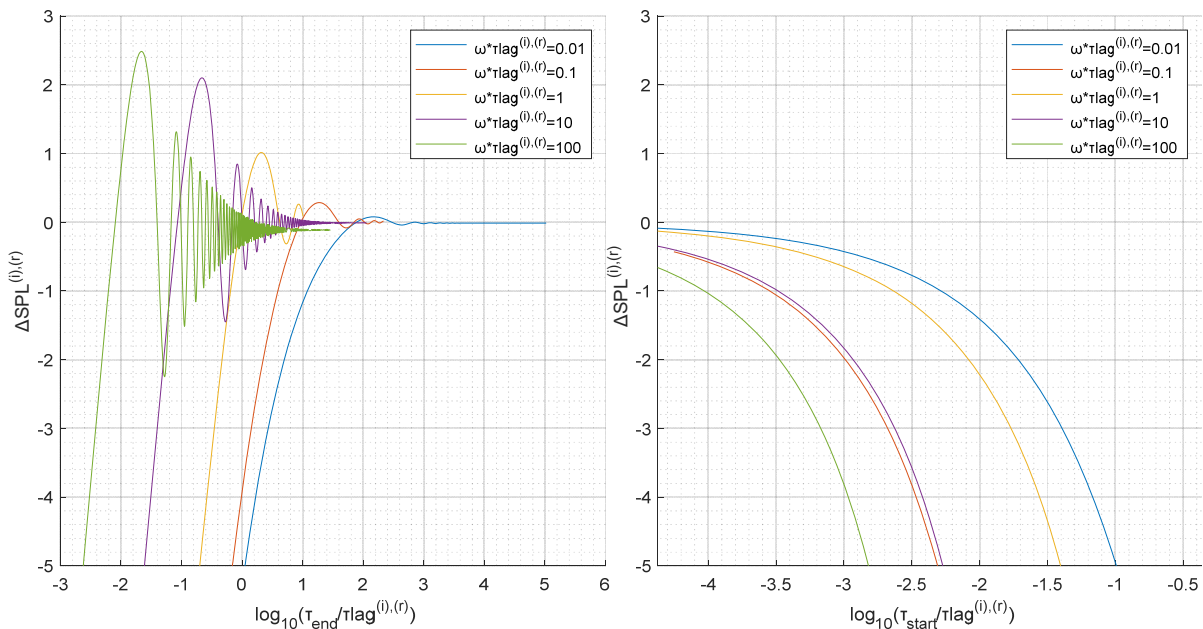


Figure 9 – Proposed families of curves that provide the correction due to the finite length of the edge, $\Delta SPL^{(i)(r)}$, versus the normalized re-radiation time for various $\omega\tau_{lag}^{(i)(r)}$ - left column: reference point on the edge – right column: reference point outside the edge.

4.3 Use of curves

The proposed curves provide the correction to the corresponding infinitely long diffracting edge for the two different terms of the diffracted field separately. Specifically, $\Delta SPL^{(i)}$ provides the correction to the term of the diffracted field associated with the incident field, while $\Delta SPL^{(r)}$ the correction to the term associated with the reflected field. For the correction to the total diffraction field, the following approximation is proposed:

$$\Delta SPL^{proposed} \cong \begin{cases} \Delta SPL^{(i)} & \text{if } \omega\tau_{tag}^{(i)} = \min(\omega\tau_{tag}^{(i)}, \omega\tau_{tag}^{(r)}) \\ \Delta SPL^{(r)} & \text{if } \omega\tau_{tag}^{(r)} = \min(\omega\tau_{tag}^{(i)}, \omega\tau_{tag}^{(r)}) \end{cases} \quad (11)$$

In other words, the correction to the total diffraction field is approximately the same to the correction of the term (incident or reflected) that has the minimum τ_{tag} . Numerical tests have been performed for a range of frequencies, source and receiver locations and lengths of finite edges and it has been concluded that in almost all cases ΔSPL provided by Eq. (11) ($\Delta SPL^{proposed}$) is very close to the ΔSPL computed analytically ($\Delta SPL^{analytical}$). Figure 10(a) shows that when the reference point is on the edge, the discrepancies between $\Delta SPL^{proposed}$ and $\Delta SPL^{analytical}$ are above 0.5 dB only for low frequencies and short segment lengths and very close to the shadow boundaries. Accordingly, for cases where the reference point is outside the edge, the discrepancies are above 1 dB in the entire region II (the region above the barrier between the two shadow boundaries) and close to the shadow boundaries.

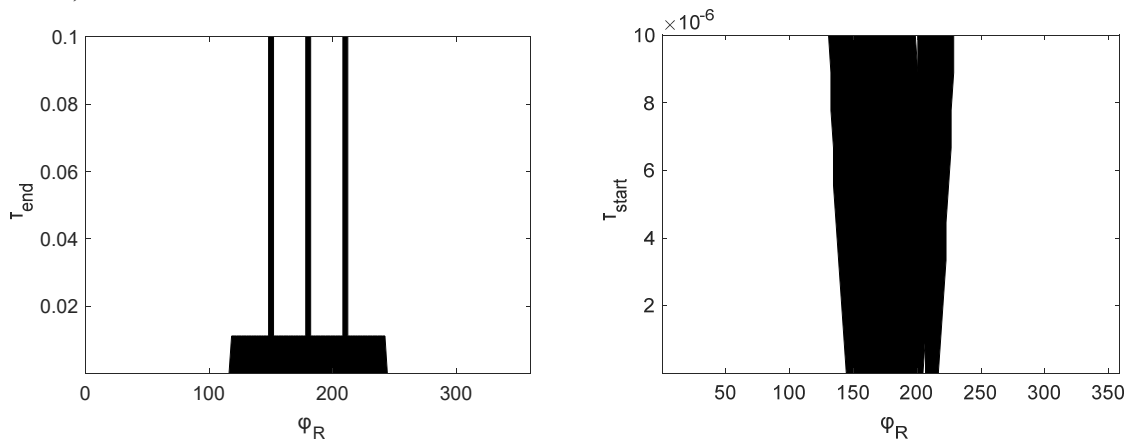


Figure 10 – Combinations of parameters (black-coloured areas) for which the proposed curves provide corrections due to finite length $\Delta SPL^{proposed}$ that differ from corrections obtained by the analytical solutions $\Delta SPL^{analytical}$ (left: reference point on the edge, right: reference point outside the edge)

Finally, we consider the case of the reference point being inside the edge, and the edge extends on both sides of the reference point (see right column of Figure 2). The edge is, thus, separated into two different edges that can be treated separately. Let $\Delta SPL^{(1)}$ be the correction obtained by the proposed curves, as described above, for the segment of the edge left of the reference point (segment $A\Xi$) and $\Delta SPL^{(2)}$ the correction for the segment of the edge to the right of the reference point (segment ΞB). The correction for the entire segment (AB) is

$$\Delta SPL_{AB} = -6 + 20 \log \left(10^{\frac{\Delta SPL^{(1)}}{20}} + 10^{\frac{\Delta SPL^{(2)}}{20}} \right) \quad (12)$$

The results obtained are in good agreement with the analytical solutions except for low frequencies, short edges and receivers in region II.

5 Conclusions

Families of curves and formulas have been derived that provide corrections due to the finite length of the diffracting edge. These corrections can be applied to the results obtained from existing methods (analytical or empirical) that predict the diffracted field around an infinitely long diffracting edge to account for the finite length of the edge.

References

- [1] Maekawa, Z. ,Noise reduction by screens, *Appl. Acoust.* ,1, 1968, pp 157-173 .
- [2] Kurze, U. J. ; Anderson, G.S. ,Sound attenuation by barriers, *Appl. Acoust.* ,4, 1971 pp 35-53 .
- [3] E. Salomons, D.; v. Maercke, J.; Defrance; Roo, F. d., The Harmonoise Sound Propagation Model, *Acust. Acta Acust* , 97, 2011, pp 62-74 .
- [4] Plovsing B. ; Kragh, J. ; Nord 2000. Comprehensive Outdoor Sound Propagation Model. Part 1: Propagation in an Atmosphere without significant Refraction, Danish Electronics, Light & Acoustics AV 1849/00, 2001.
- [5] Hadden W.J.; Pierce, A.D. Sound diffraction around screens and wedges for arbitrary point source locations, *J. Acoust. Soc. Am.* , 69,1981,pp 1266-1276 .
- [6] U.P. Svensson. P; P.T Calamia ; Nakanishi, S . Frequency-Domain Edge Diffraction for Finite and Infinite Edges , *Acust. Acta Acust* , 95 ,2009, pp 568-572.
- [7] Nikolaou, P., *A contribution to the theoretical study and numerical calculation of edge diffraction*, PhD diss, University of Patras. Patras (Greece), 2019.
- [8] Nikolaou, P., Menounou, P. “Analytical solution for diffraction by finite edges in frequency domain,” Euronoise 2021, Madeira, Portugal, October 25-27, 2021
- [9] Corless, R. M.,; Gonnet, G. H.,; Hare, D. E. G., Jeffrey, D. J.,; Knuth, D. E. On the Lambert W Function. *Advances in Computational Mathematics*, Vol. 5, 1996, pp. 329–359.
- [10] Menounou, P. A correction to Maekawa’s curve for the insertion loss behind barriers , *J. Acoust. Soc. Am*,110,2001,pp 1828-1838.